Relativistic Electron Beam Transport for Fast Ignition Relevant Scenarios

WCI
WEAPONS
AND COMPLEX
INTEGRATION

Larissa A. Cottrill

Thesis Defense

Massachusetts Institute of Technology

January 27, 2009

Option: Auspice statement or other directorate information

Lawrence Livermore National Laboratory

This document was prepared as an account of work sponsored by an agency of the United States government. Neither the United States government nor Lawrence Livermore National Security, LLC, nor any of their employees makes any warranty, expressed or implied, or assumes any legal liability or responsibility for the accuracy, completeness, or usefulness of any information, apparatus, product, or process disclosed, or represents that its use would not infringe privately owned rights. Reference herein to any specific commercial product, process, or service by trade name, trademark, manufacturer, or otherwise does not necessarily constitute or imply its endorsement, recommendation, or favoring by the United States government or Lawrence Livermore National Security, LLC. The views and opinions of authors expressed herein do not necessarily state or reflect those of the United States government or Lawrence Livermore National Security, LLC, and shall not be used for advertising or product endorsement purposes.

This work performed under the auspices of the U.S. Department of Energy by Lawrence Livermore National Laboratory under Contract DE-AC52-07NA27344.

Summary

PIC simulations and analytical models have been used to explore hot electron transport for fast ignition

WCI WEAPONS AND COMPLEX INTEGRATION

- Central to the feasibility of fast ignition is the transport of a relativistic electron beam through dense plasma
- The cone-guided fast ignition scheme will involve hot electron transport in 2 phases:
  - Hot electron production followed by transport along the cone wall
  - Beam propagation from the cone tip to a high density, compressed core
- Novel research results will be shown in 3 areas
  - Electron surface confinement and the escaping electron phenomenon
  - Kinetic and collisional effects on the linear evolution of relevant beam instabilities
  - Effects of nonlinear beam instability saturation on electron transport

We have attributed enhanced surface emission measurements to target geometry, not surface confinement

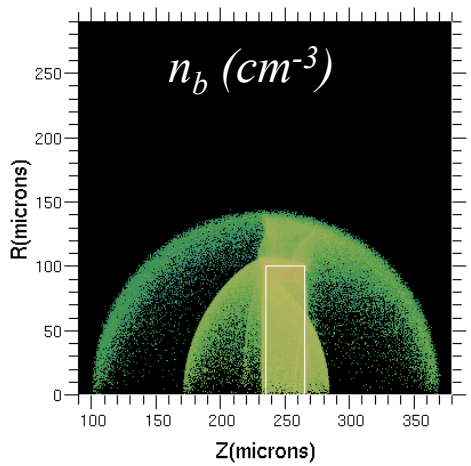

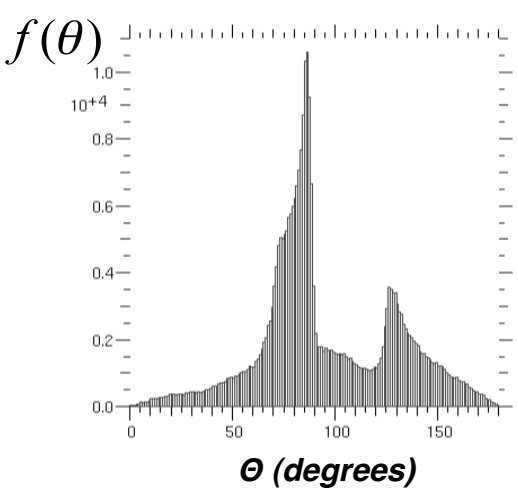

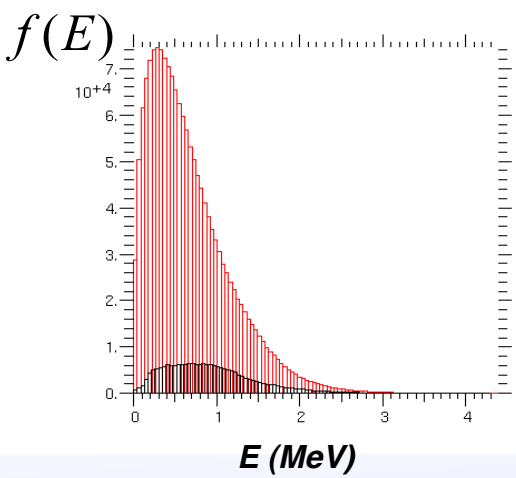

- Strong electrostatic fields alter measured hot electron distributions
- Measured spectrums have been found to depend on target geometry …not initial birth distributions or surface electromagnetic fields
- Measured spectrums are significantly harder than birth spectrums

We have investigated kinetic and collisional effects on the linear evolution of FI relevant beam instabilities

WCI WEAPONS AND COMPLEX INTEGRATION

Growth rates computed for various theoretical distributions

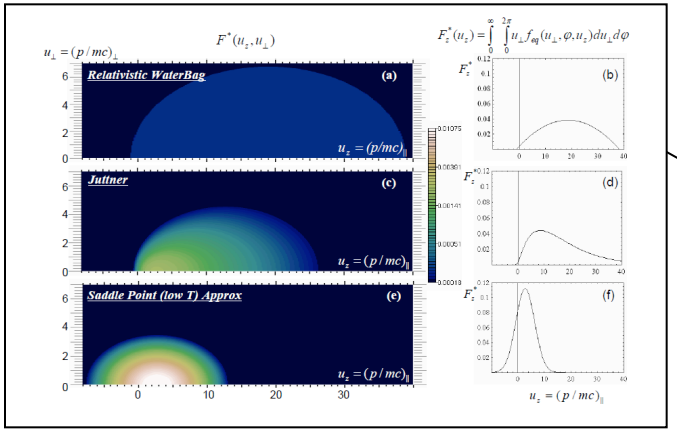

Collisional Effects

Vlasov + Krook operator

$$\sum_s \frac{\partial f_s}{\partial t} + \vec{v}\cdot\frac{\partial f_s}{\partial \vec{r}} + q\left(\vec{E} + \frac{\vec{v}}{c}\times\vec{B}\right)\cdot\frac{\partial f_s}{\partial \vec{p}} = -\nu_{pei}\left\{f_{pe} - n_{pe} f_{pe}^0\right\}$$

Fast Ignition Relevant Beam Instabilities

- Two-stream
- Weibel
- Filamentary

Fit obtained from explicit PIC simulation of the LPI

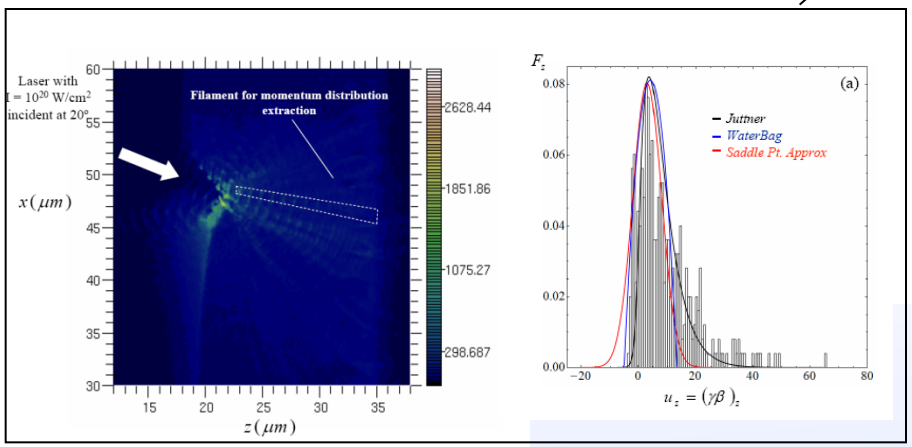

Growth rates for fit parameters

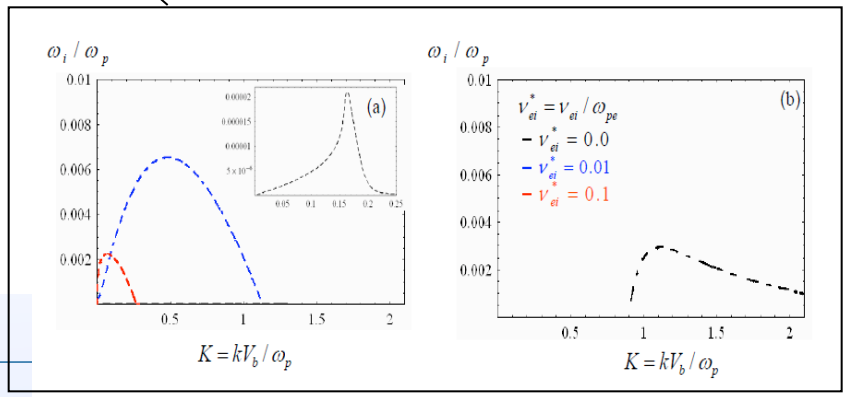

Analysis of the nonlinear regime reveal that instabilities are of little concern for fast ignition parameters

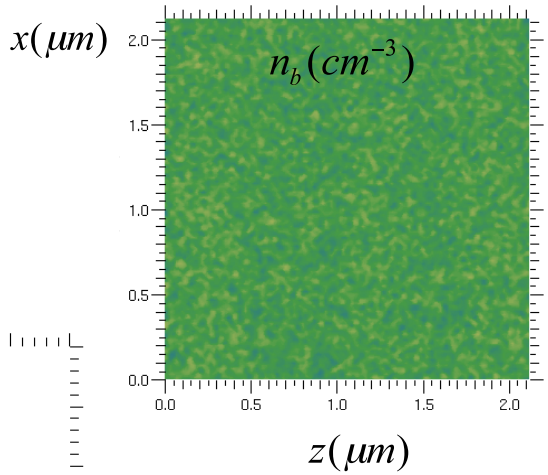

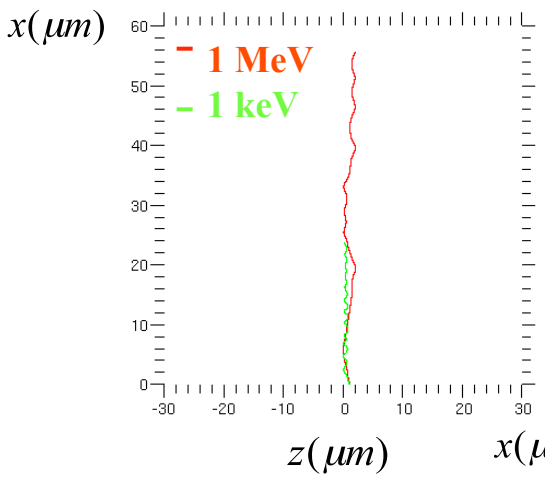

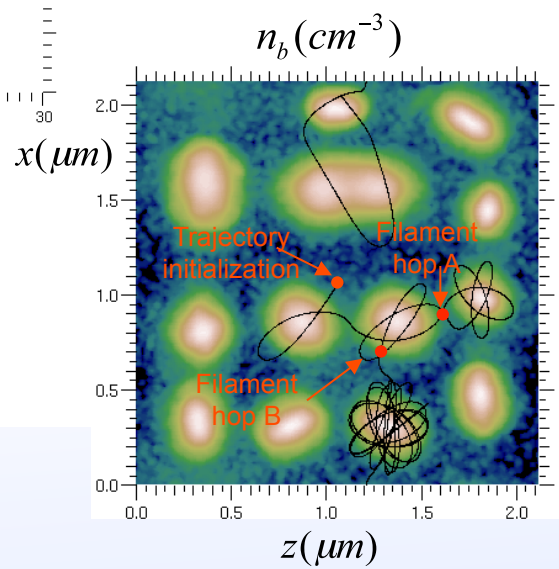

- Minimal filamentation is observed in simulations using the explicit fit parameters
- Particle trajectories appear relatively straight over the particle range
- A random “filament hopping” phenomenon was observed from particle trajectories

Fast Ignition is a novel alternative to the conventional method of hot spot inertial fusion

WCI WEAPONS AND COMPLEX INTEGRATION

Initial compression via long, moderate intensity laser pulse

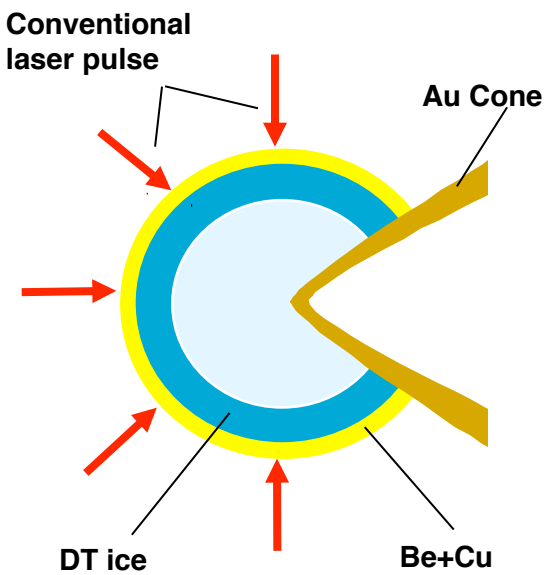

Ignition via a short, high intensity laser pulse

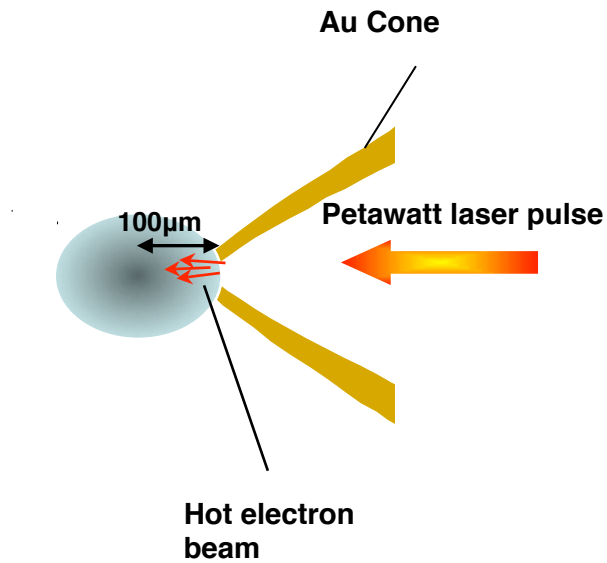

Goal: Propagate a relativistic electron beam ~ 100μm through dense plasma to n ~ 10^{26} cm^{-3}

Electron transport from the cone surface will include physics at multiple spatial and time scales

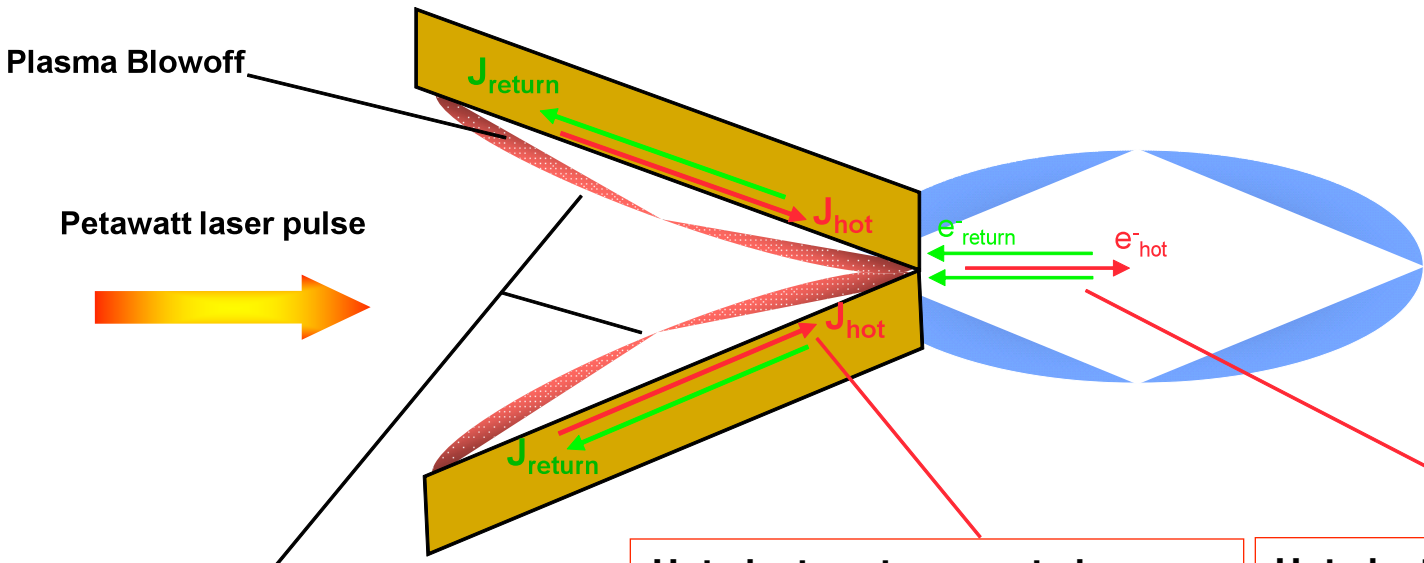

Laser-Plasma Interaction

- Modeled with explicit PIC codes (Z3)
- High spatial & temporal resolution (resolves Debye length/ plasma frequency)
- Used to extract hot electron distribution

Hot electron transport along cone wall

- Modeled with implicit PIC codes (LSP)
- Lower spatial & temporal resolution needed (does not resolve Debye length/ plasma frequency)
- Used to determine optimal cone design for maximum surface current

Hot electron transport to core

- Modeled with implicit PIC (not feasible for FI density)
- Basic physics can be gained from simpler models (explicit PIC /analytics)
- High spatial & temporal resolution
- Used to determine beam stability

The LSP code has served as a key numerical tool for understanding electron transport in the various regimes

WCI WEAPONS AND COMPLEX INTEGRATION

- LSP is a 3D/3V electromagnetic hybrid particle-in-cell (PIC) code with relativistic and collisional effects
- Explicit algorithm
  - Used to model sub-micro-scale electron transport (instability growth)
  - Resolution of the plasma frequency and Debye length
  - Utilizes the classic leap-frog particle-push
  - Has been benchmarked with theory
- Hybrid implicit algorithm
  - Used to model multi-micro-scale electron transport
  - Does not resolve plasma frequency and Debye length
  - Utilizes hybrid implicit particle-push (hot e^- kinetic; background e^-)
- Collision Model
  - A new Langevin-based formalism has been added1
  - Includes velocity-dependent friction and diffusion coefficients and relativistic effects

Recent publications have claimed that electromagnetic fields confine and guide electrons along the surface

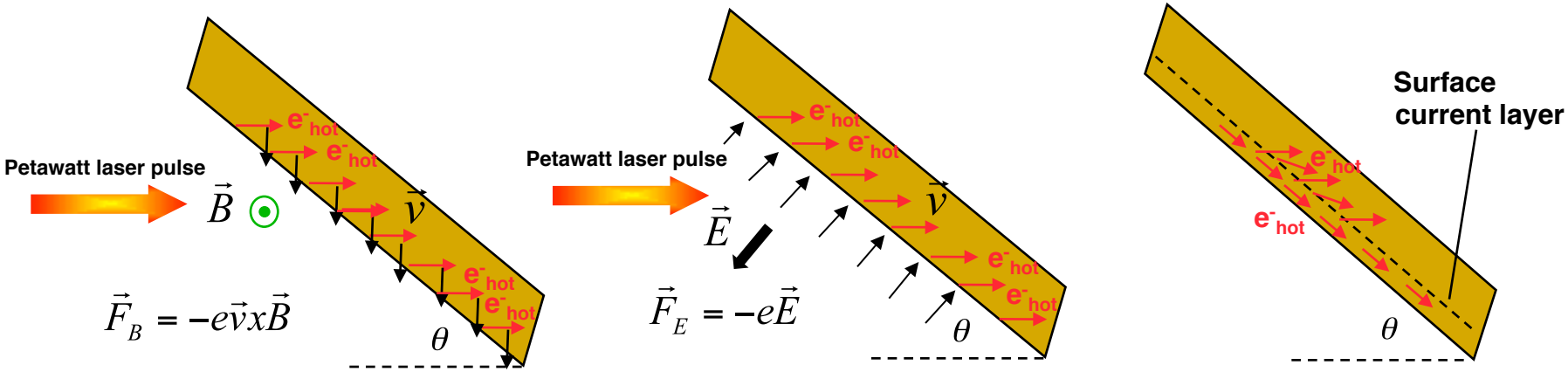

- Hot electrons are injected into the plasma via collective absorption mechanisms (JxB heating, Brunel, resonance abs., etc.)
- Accelerated electrons induce magnetic fields along the cone surface
- When the magnetic field is sufficiently intense, some electrons are reflected back to the vacuum
- These electrons are reflected back again from the vacuum region by the negative space charge

The Confinement Conundrum

WCI WEAPONS AND COMPLEX INTEGRATION

Nakamura et al., 2004

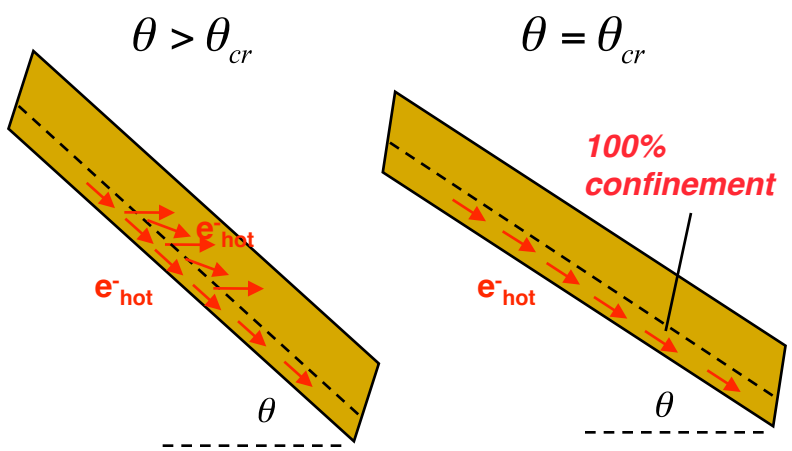

- Analytical/PIC study
- Claims a critical angle exists below which all electrons are confined to surface

Li et al., 2006

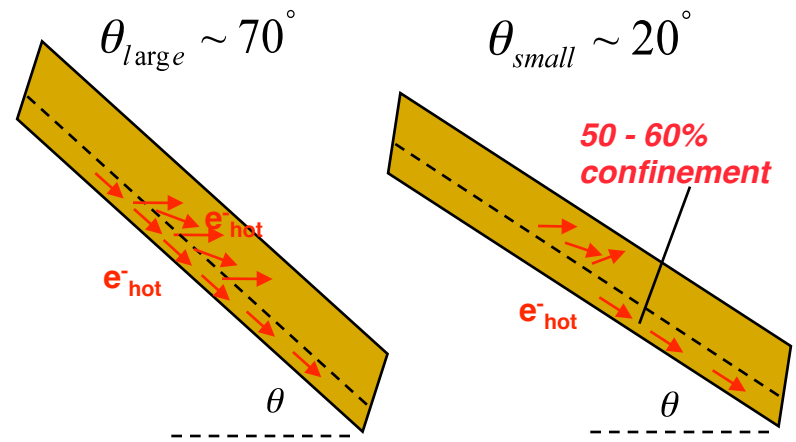

- Experimental/PIC study
- Claims no critical angle but substantial increase in confinement at small angles of incidence

LSP and conventional PIC simulations suggest that both of these claims are exaggerated

LSP simulations reveal much smaller surface fractions than previously reported results

- Electrons were promoted from the background to mimic the laser from Li et al.
  - 30 fs Gaussian pulse
  - 10 μm spot size
  - 0.3 J of energy (~50% of laser energy from Li et al.)
  - 305 keV drifting Jüttner distribution

LSP Geometry

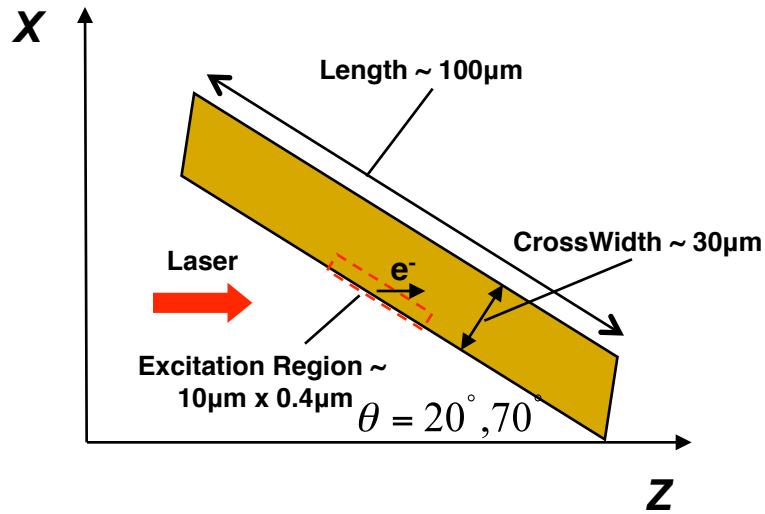

Simulation	Fraction of hot electrons traveling down the surface	Fraction of energy carried down the surface
Al slab (no collisions)	8.2%	5.5%
Al slab (collisions)	12.5%	9.1%
Al cone (no collisions)	6.9%	4.9%

Particle trajectories along the surface suggest that confinement is limited to selected energies & angles

WCI WEAPONS AND COMPLEX INTEGRATION

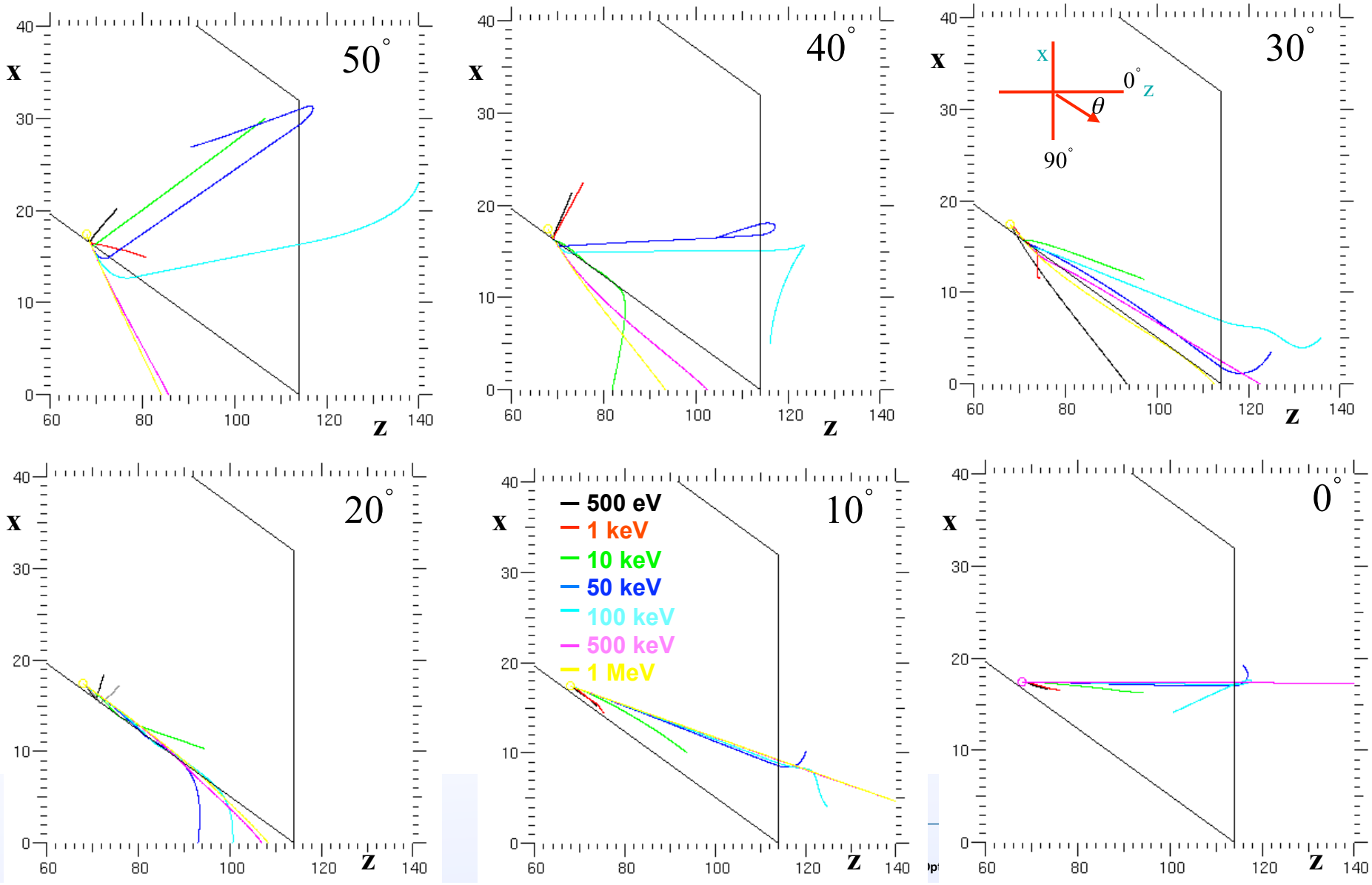

We have linked the discrepancy between experimental and PIC results to the escaping electron phenomenon

WCI WEAPONS AND COMPLEX INTEGRATION

- The "escaping electron" phenomenon refers to significant differences in the measured (escaping) hot electron spectrum with respect to the original birth spectrum due to the generation of strong electrostatic self-fields

- LSP results show that enhanced surface emission is due to target geometry, not surface confinement or laser incidence angle

- Lower potential drop across the top edge creates a preferred path of least resistance

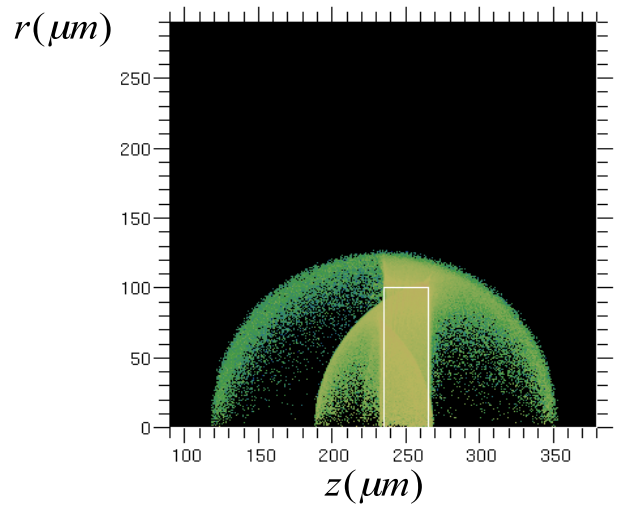

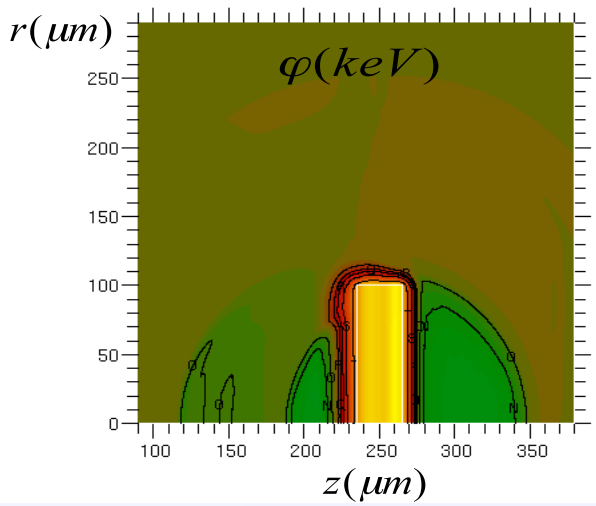

Determination of escaping electrons and surface escape fraction

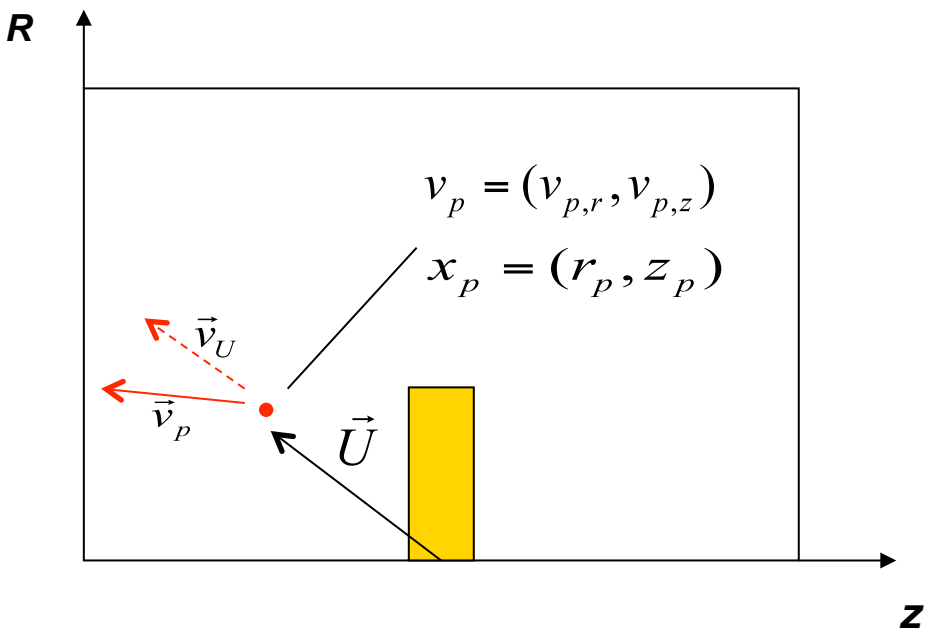

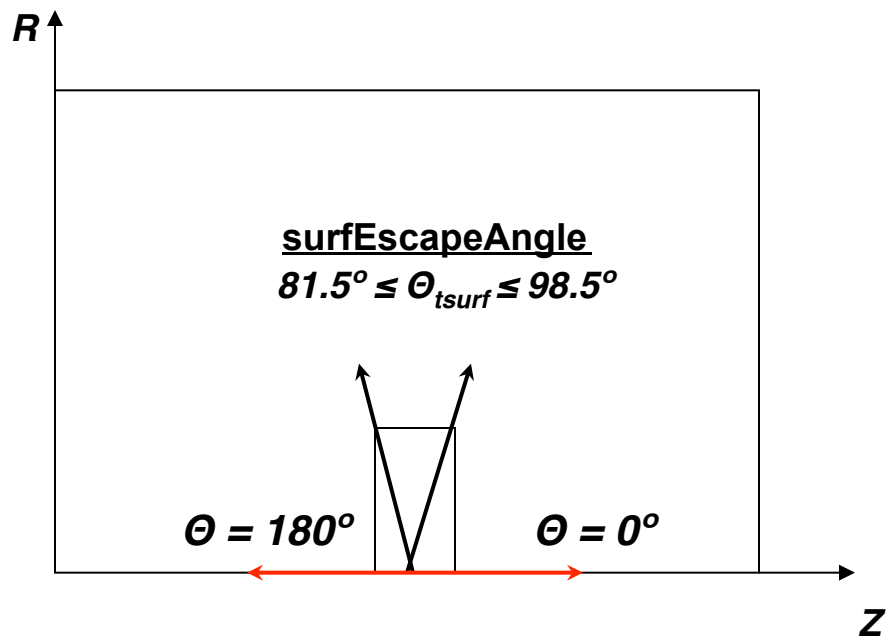

$$v_U = \vec{v}_p \cdot \vec{U} \longrightarrow \gamma_U$$

$$E_U = mc^2(\gamma_U - 1) \begin{cases} \text{If } E_U > \varphi(r_p, z_p) \text{.....escape} \\ \text{If } E_U < \varphi(r_p, z_p) \text{.....no escape} \end{cases}$$

$$surf\ EscapeFrac = \frac{\#\text{electrons within } 81.5^\circ \le \Theta_{tsurf} \le 98.5^\circ}{\text{total \# of escape electrons}}$$

Effects of target size

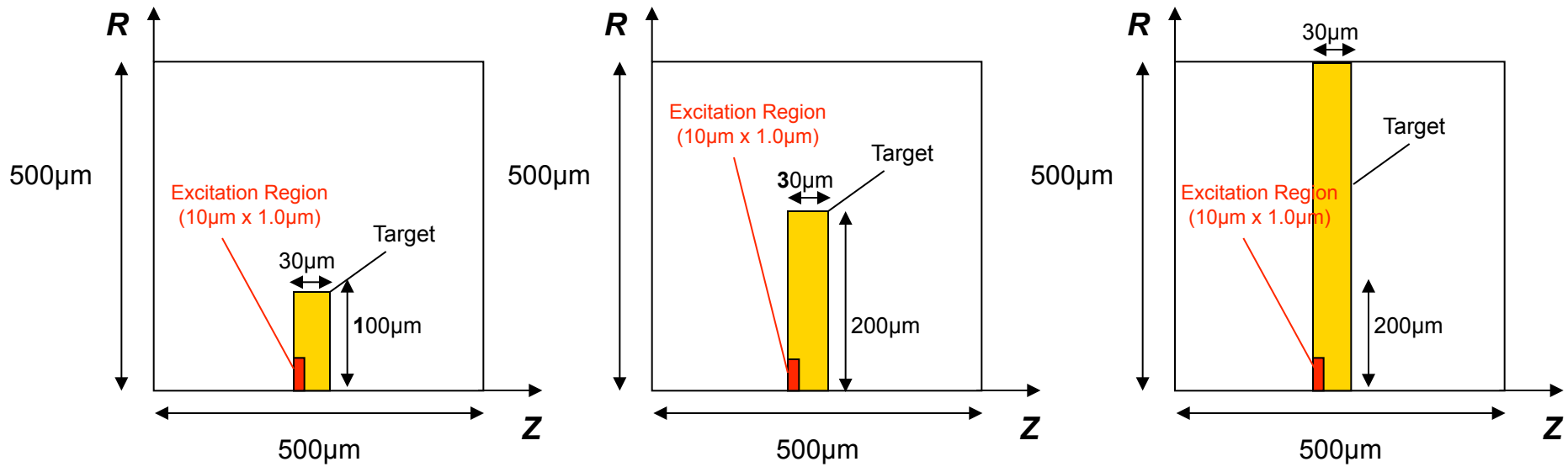

Effects of Target size results

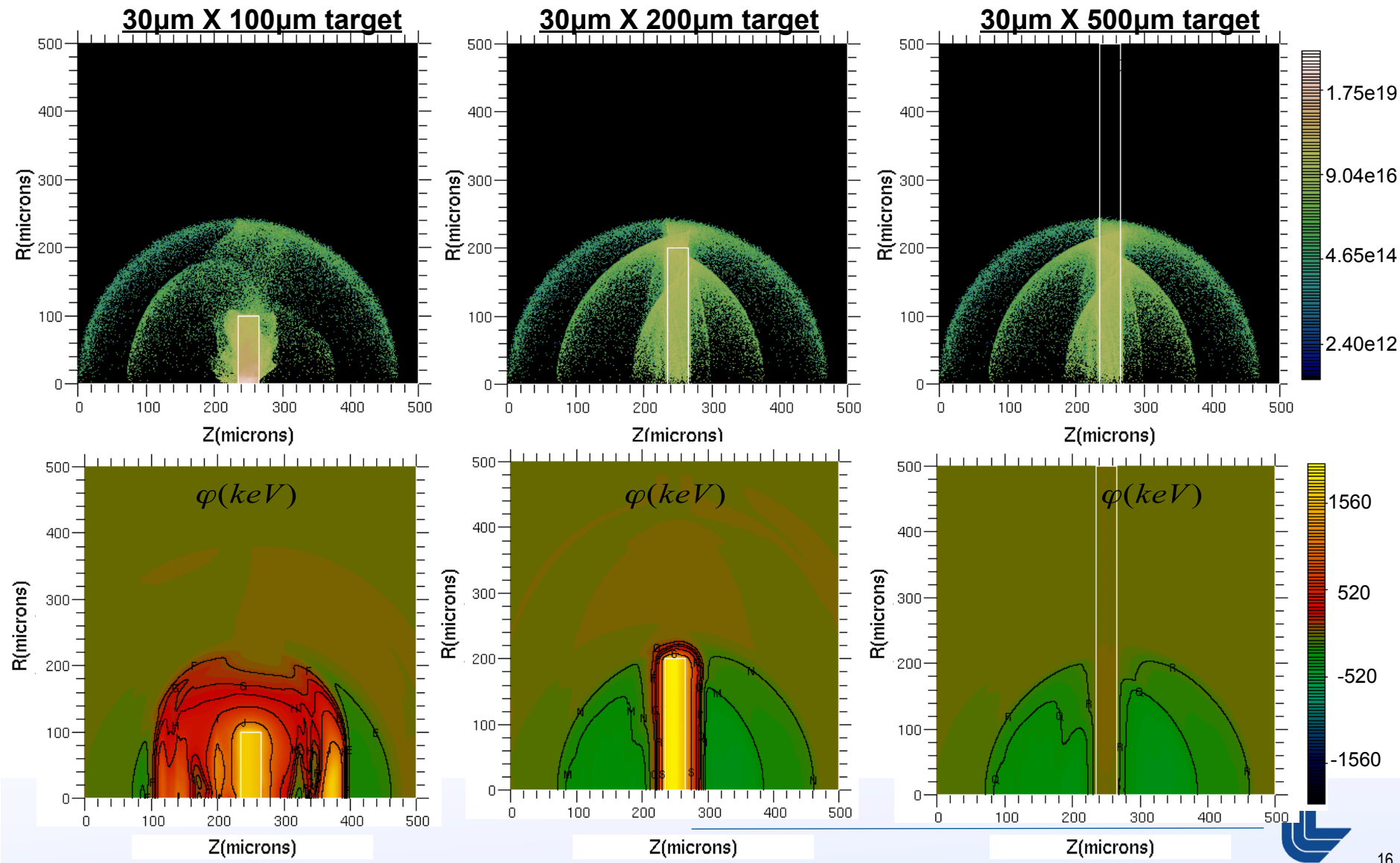

Effects of target size results

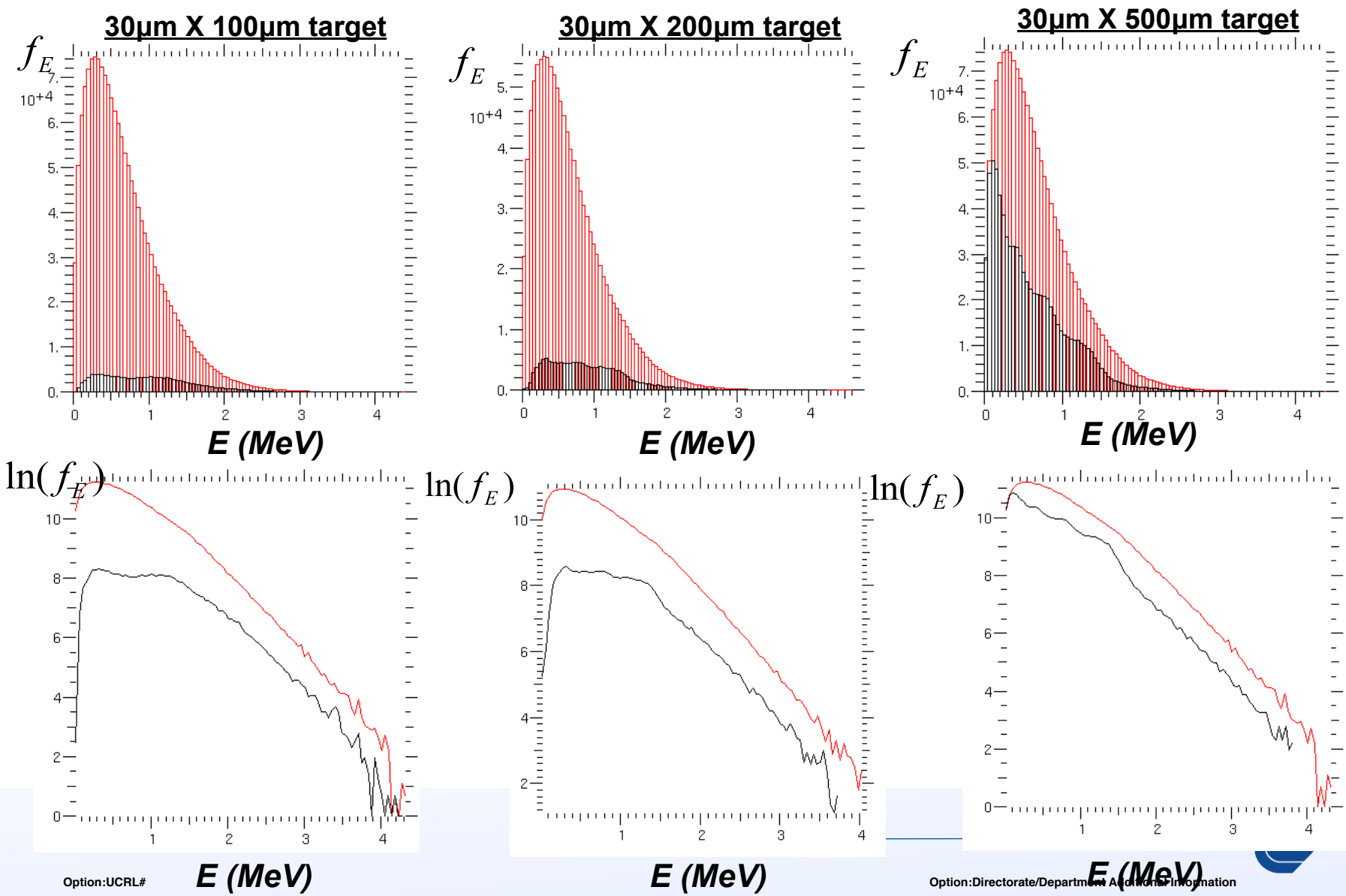

Effects of Angular Orientation/Results

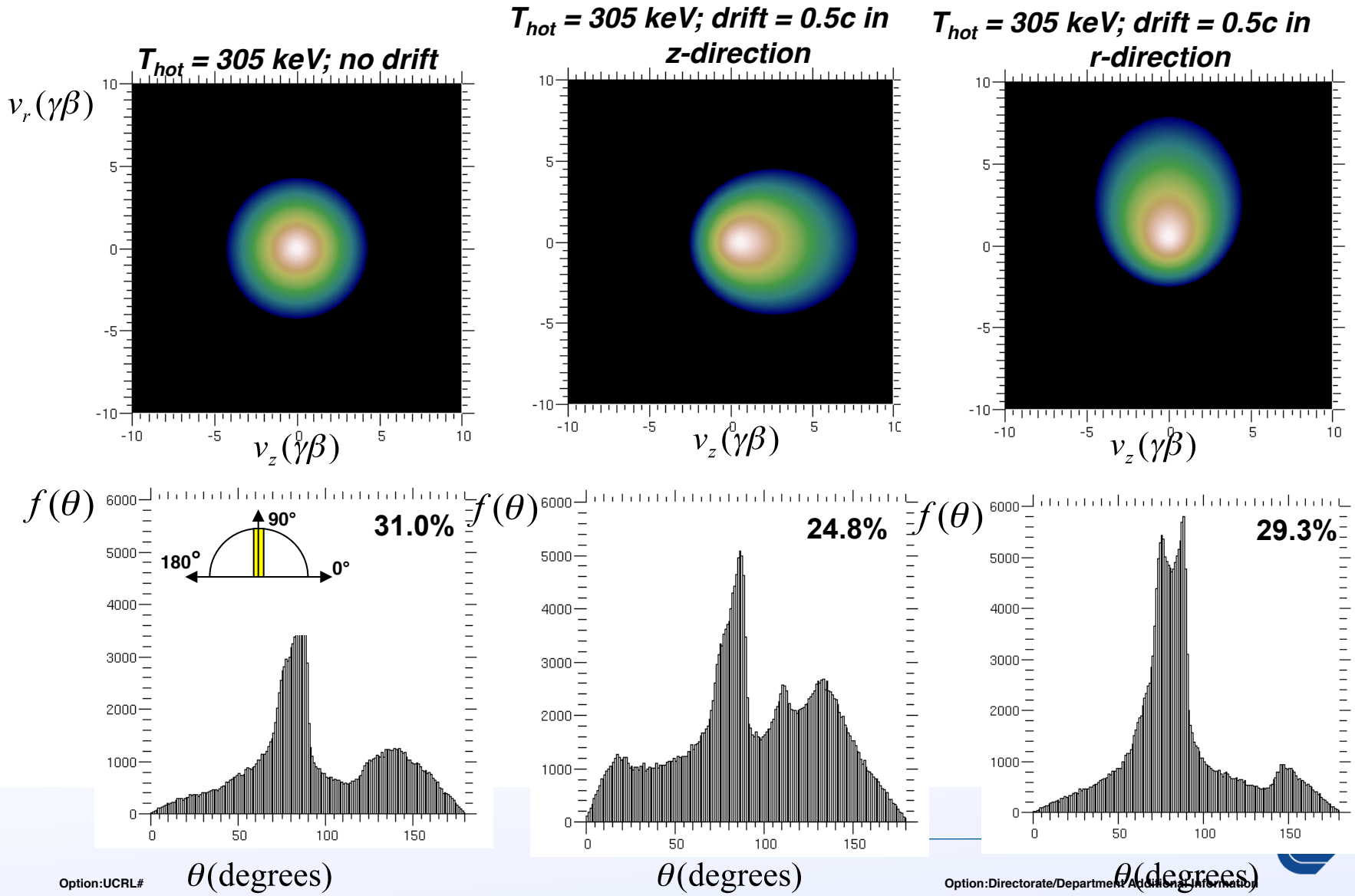

PIC simulations and analytical models were used to explore kinetic and collisional effects on instability growth

WCI WEAPONS AND COMPLEX INTEGRATION

- A relativistic electron beam propagating through dense plasma is subject to instabilities that act to inhibit transport
  - Two-stream
  - Weibel
  - Filamentary
- Collisions and the form of the initial distribution will affect the evolution of these instabilities
- Analytical calculations of instability growth rates will be presented in the collisional and collisionless limits for several distributions
  - Relativistic WaterBag
  - Relativistic Maxwellian (Juttner)
  - Saddle Point (low temperature approx. to Juttner)
  - Distribution from an explicit PIC simulation of the laser plasma interaction

Critical beam instabilities relevant for fast ignition

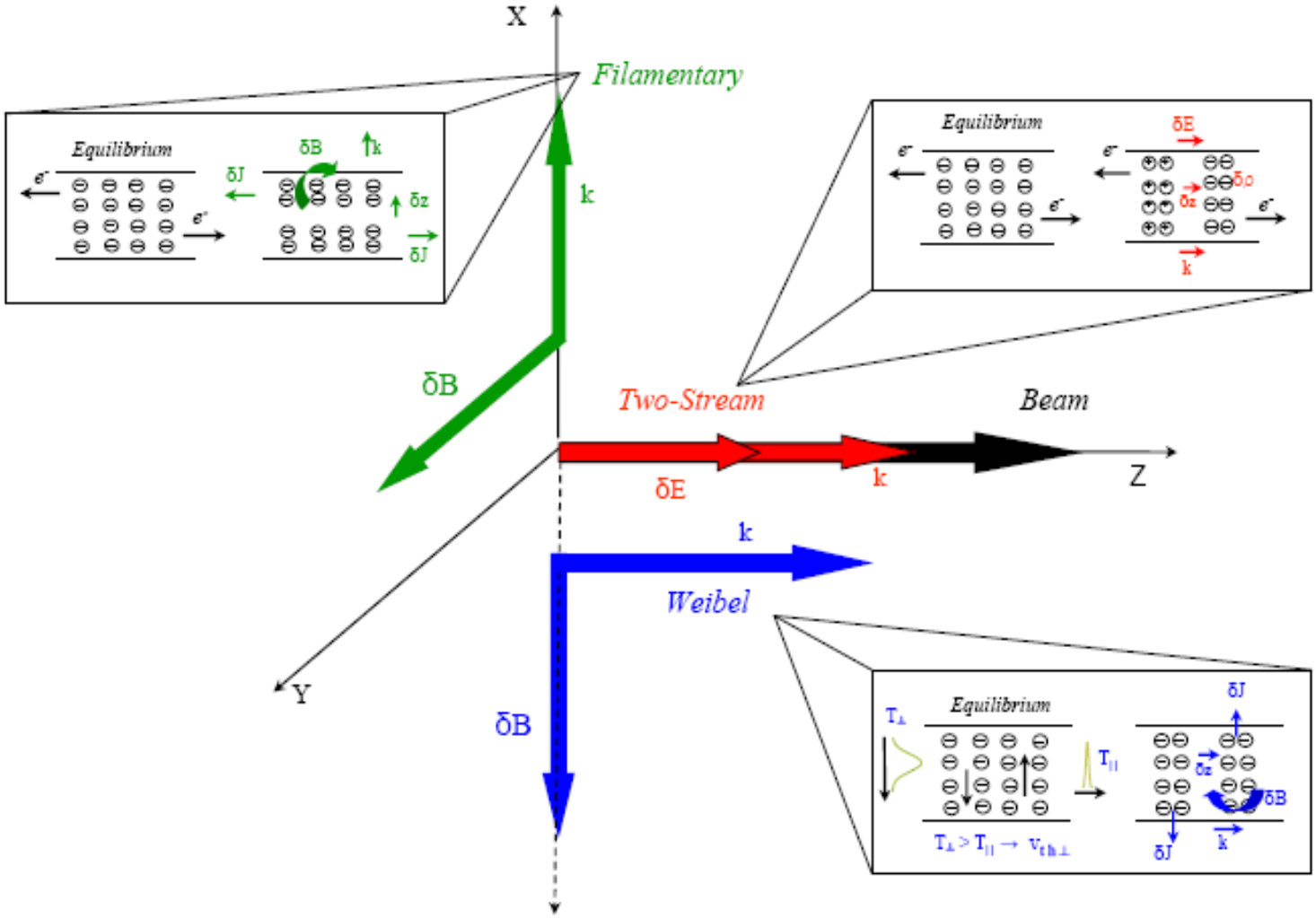

For analytical growth rate calculations, an equilibrium Vlasov model is used with a simple collision operator

WCI WEAPONS AND COMPLEX INTEGRATION

- Equilibrium model assumptions:
  - Applicable in the linear growth regime (density gradients are not yet felt)
  - Immobile ions
  - Charge and current neutrality
  - $T_\perp \not> T_{||} \rightarrow$ Weibel instability is stable
  - $a = n_b/n_p = 0.1$
  - Only background electron-ion collisions (n_{pei}) are important
- Collisionality is included with a simple BGK-type formulation

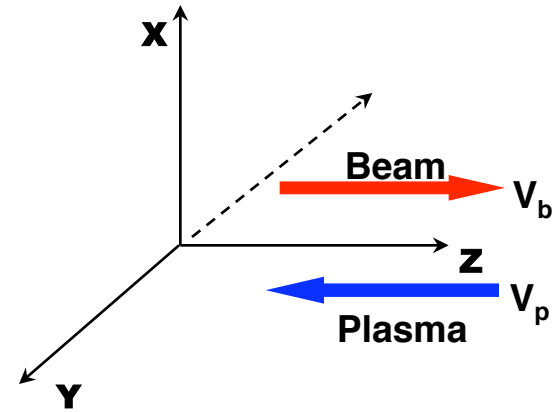

Vlasov + Krook operator

$$\sum_s \frac{\partial f_s}{\partial t} + \vec{v}\cdot\frac{\partial f_s}{\partial \vec{r}} + q\left(\vec{E} + \frac{\vec{v}}{c}\times\vec{B}\right)\cdot\frac{\partial f_s}{\partial \vec{p}} = -\nu_{pei}\left\{f_{pe} - n_{pe} f_{pe}^0\right\}$$

We have explored three theoretical distributions thought to resemble the hot electron beam distribution

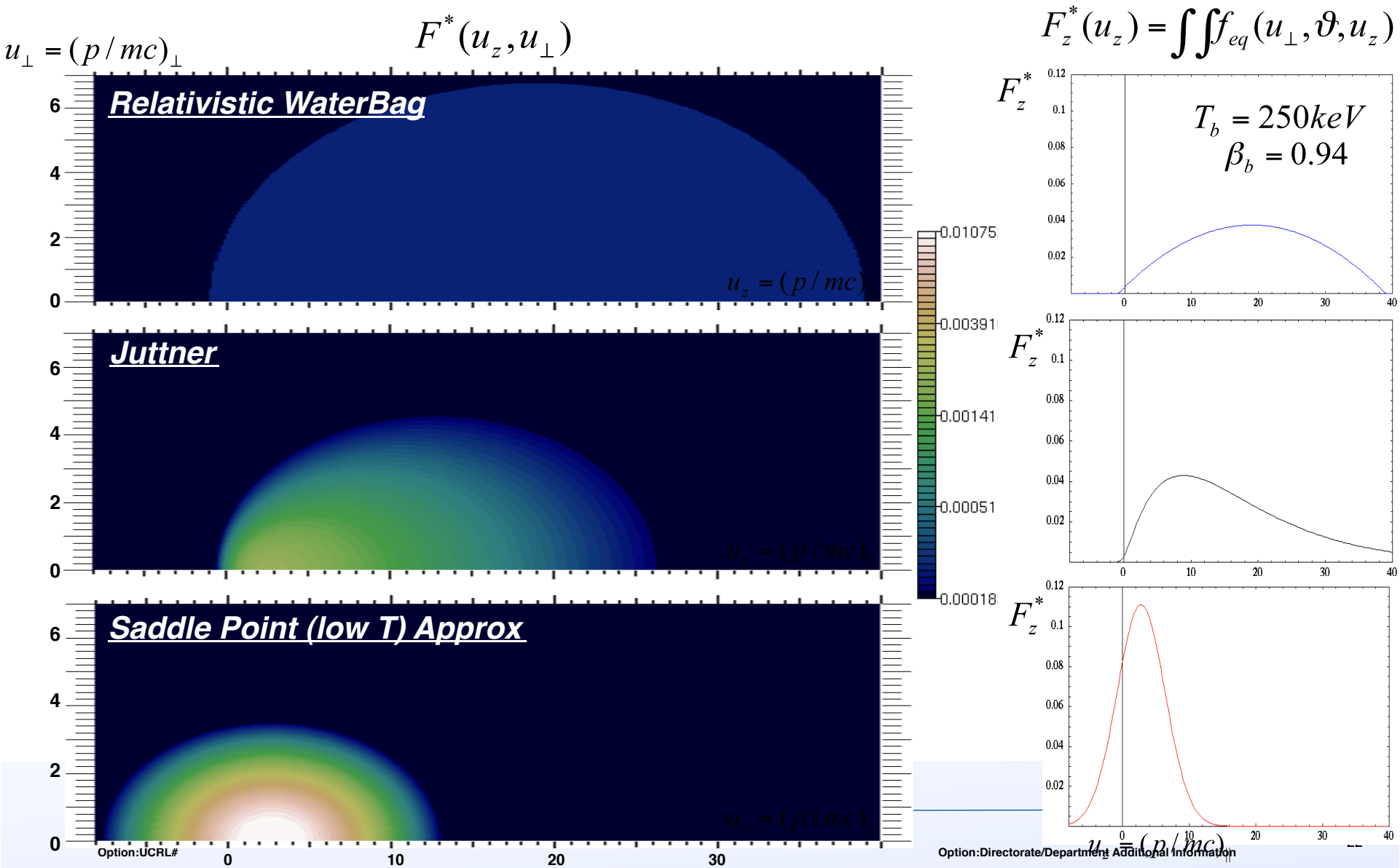

Two stream results

Filamentary results

Plasma density effects

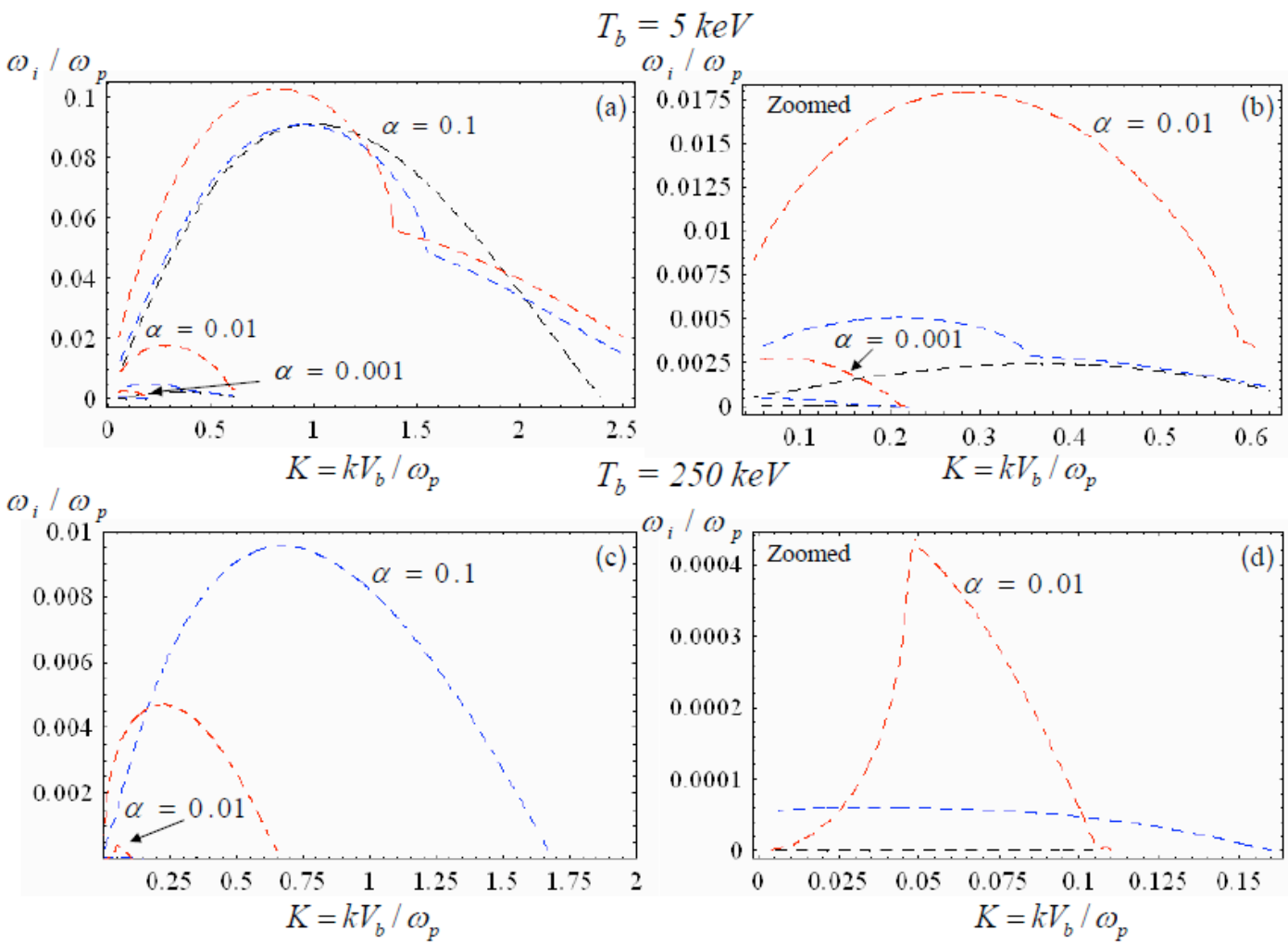

2D Explicit PIC simulations of a short high intensity LPI show a best fit with a Jüttner distribution

Density of electrons with $\gamma > 2$

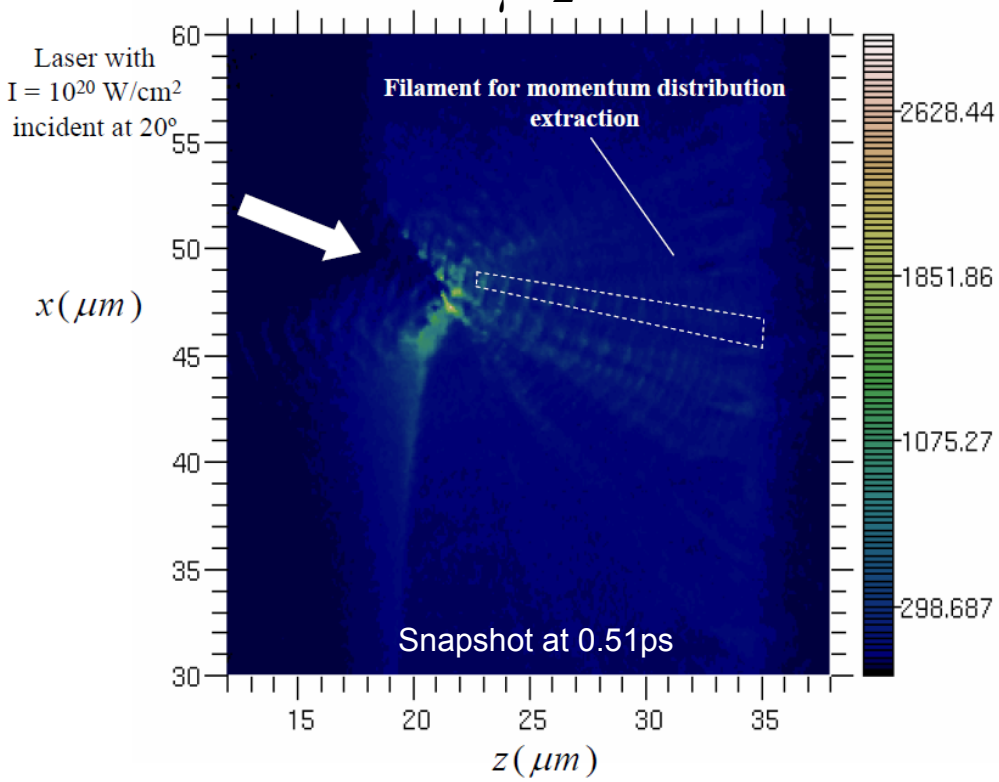

Longitudinal Momentum

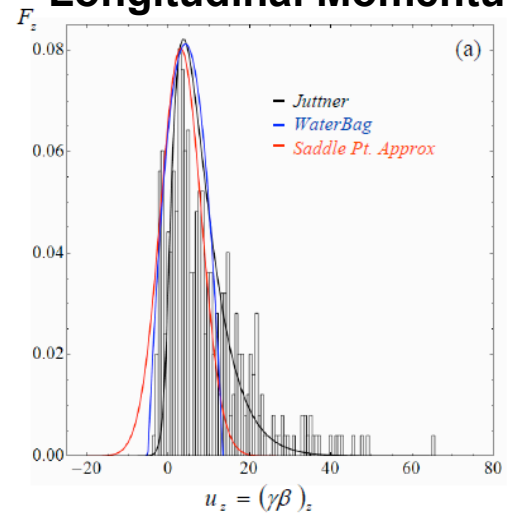

Transverse Momentum

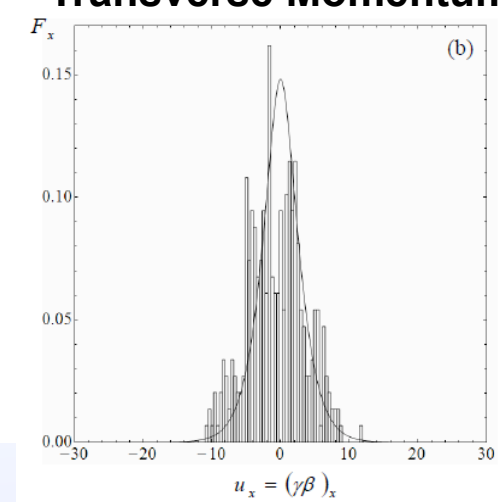

Juttner Fit Parameters to PIC data:

$$T_b = 531 keV, \beta_b = 0.76$$

Z3 Simulation courtesy of B. F. Lasinski

Growth rates for fit data parameters

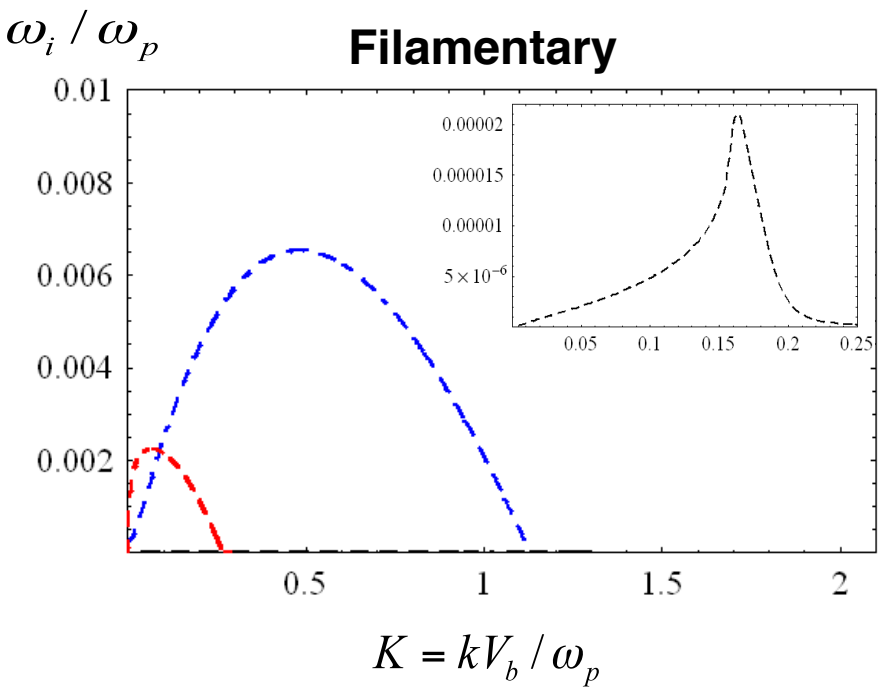

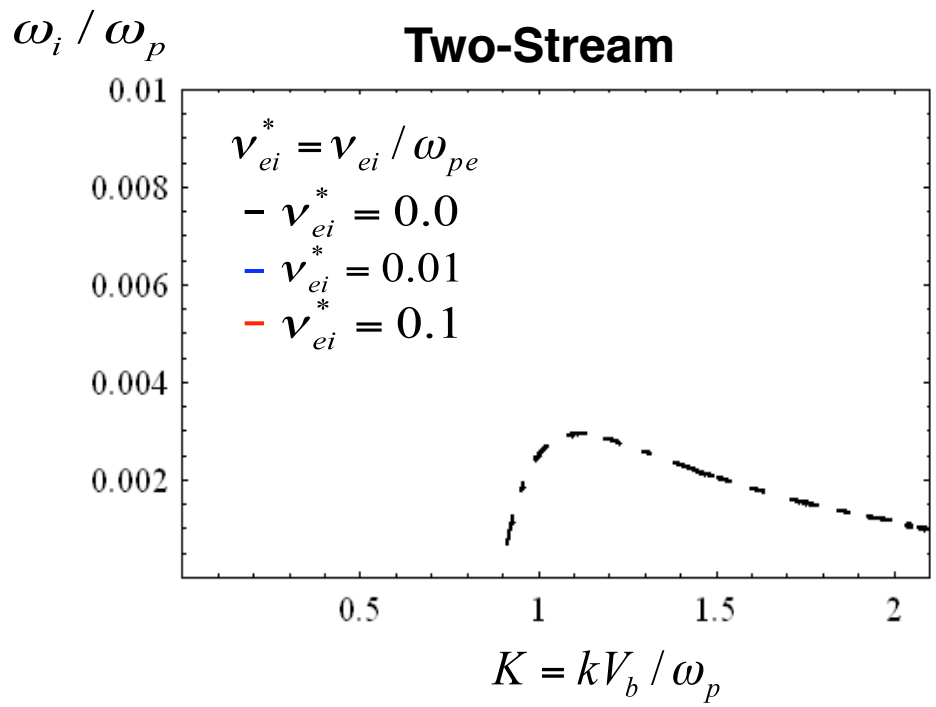

The saturated state of the instabilities will ultimately dictate how efficiently electrons will be transported to the core

WCI WEAPONS AND COMPLEX INTEGRATION

- Early work by Manheimer and Davidson attributed saturation to the process of "magnetic trapping"
  - Magnetic field perturbations grow to reach a sufficient level that the gyro-radius of electrons become small enough that they become trapped in the potential well
  - As more and more particles become trapped, less and less energy gets fed into the wave and instability growth ceases
  - This point of stabilization was found to occur when

$$\omega_{Bounce} = \sqrt{\left|\frac{ekV\overline{B}}{mc}\right|} \sim \gamma$$

- The goal of this work is to under stand the effects of the initial beam-plasma state and collisions on magnetic trapping and B_{sat}

Problem setup/different cases

- 4 Equilibrium cases were considered…
  A. T_b = 5 keV; β_b = 0.94; no collisions
  B. T_b = 5 keV; β_b = 0.94; collisions
  C. T_b = 531 keV; β_b = 0.94; no collisions
  D. T_b = 531 keV; β_b = 0.94; collisions

- …for 2 different beam-to-plasma density ratios $\alpha = n_b/n_p = 0.1, 0.1$

- PIC parameters
  — 100 particles-per-cell
  — 31 cells per λ
  — 20 time steps per plasma period
  — Explicit PIC algorithm
  — Manheimer collision model
  — Jüttner beam distribution

PIC Geometry

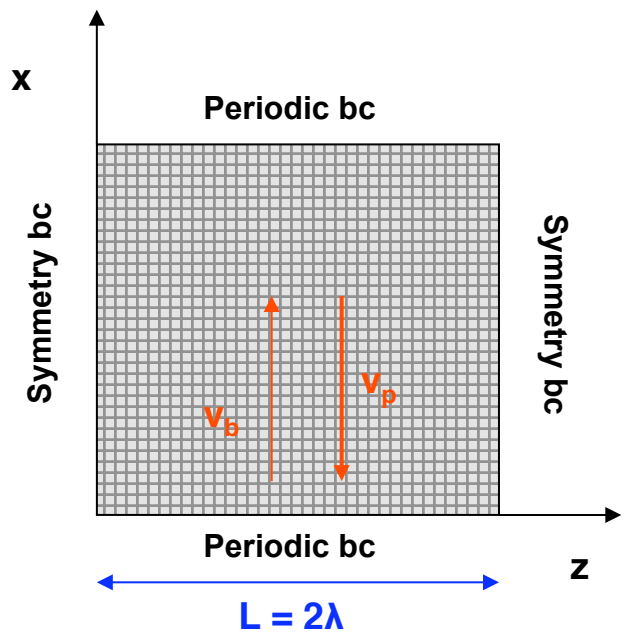

Alpha = 0.1 cases

WCI WEAPONS AND COMPLEX INTEGRATION

$\omega_p t = 200$ $\omega_p t = 500$ $\omega_p t = 1025$

A:
T_b = 5keV; β_b = 0.94;
no collisions

B:
T_b = 5keV; β_b = 0.94;
collisions

C:
T_b = 531keV; β_b = 0.76;
no collisions

D:
T_b = 531keV; β_b = 0.76;
collisions

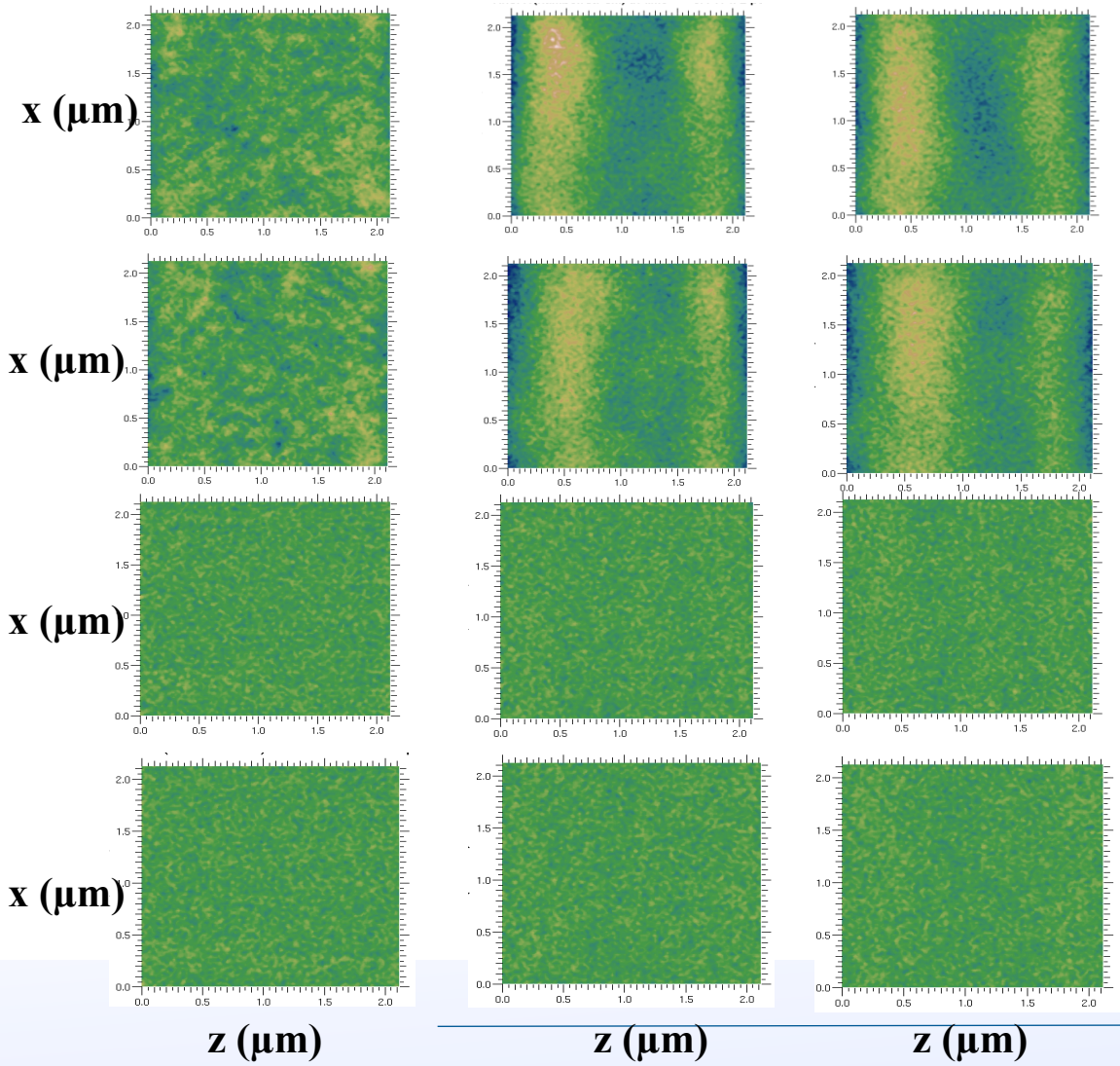

Alpha = 0.01 cases

WCI WEAPONS AND COMPLEX INTEGRATION

$\omega_p t = 200$ $\omega_p t = 500$ $\omega_p t = 1025$

E:
T_b = 5keV; β_b = 0.94;
no collisions

F:
T_b = 5keV; β_b = 0.94;
collisions

G:
T_b = 531keV; β_b = 0.76;
no collisions

H:
T_b = 531keV; β_b = 0.76;
collisions

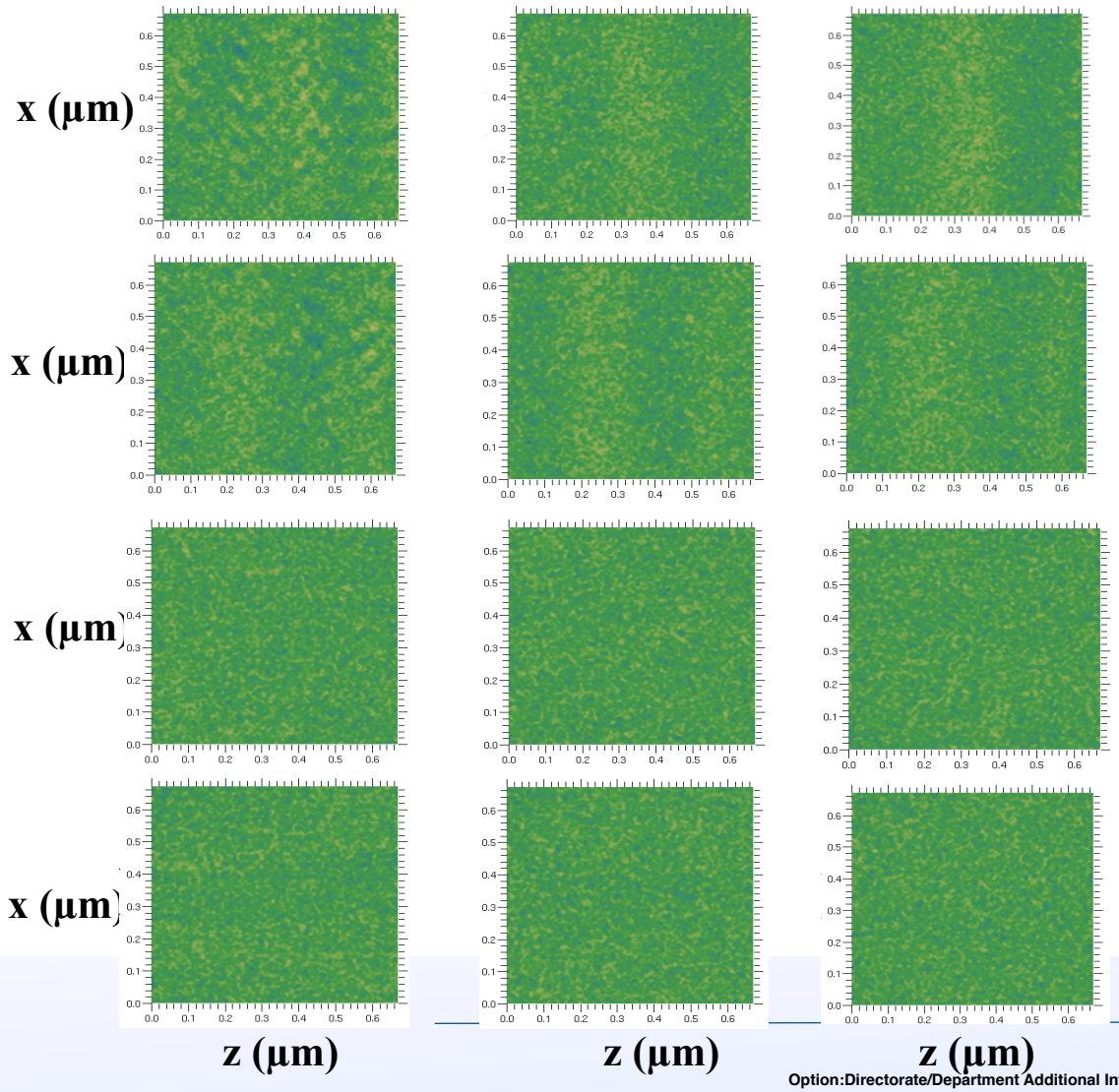

	Case	γ	B_{sat}
$\alpha = 0.1$	A **T_b = 5keV; β_b = 0.94; no collisions**	0.101	3.05×10^7
	B **T_b = 5keV; β_b = 0.94; collisions**	0.101	2.92×10^7
	C **T_b = 5keV; β_b = 0.94; collisions**	0.00002	1.04×10^7
	D **T_b = 531keV; β_b = 0.76; collisions**	0.0065	1.05×10^7
$\alpha = 0.01$	E **T_b = 5keV; β_b = 0.94; no collisions**	0.0024	1.02×10^7
	F **T_b = 5keV; β_b = 0.94; collisions**	0.0051	9.92×10^6
	G **T_b = 5keV; β_b = 0.94; collisions**	0.00000064	3.30×10^6
	H **T_b = 531keV; β_b = 0.76; collisions**	0.000024	3.13×10^6

Cold trajectories/pathlengths

Aspect Ratio 1:26

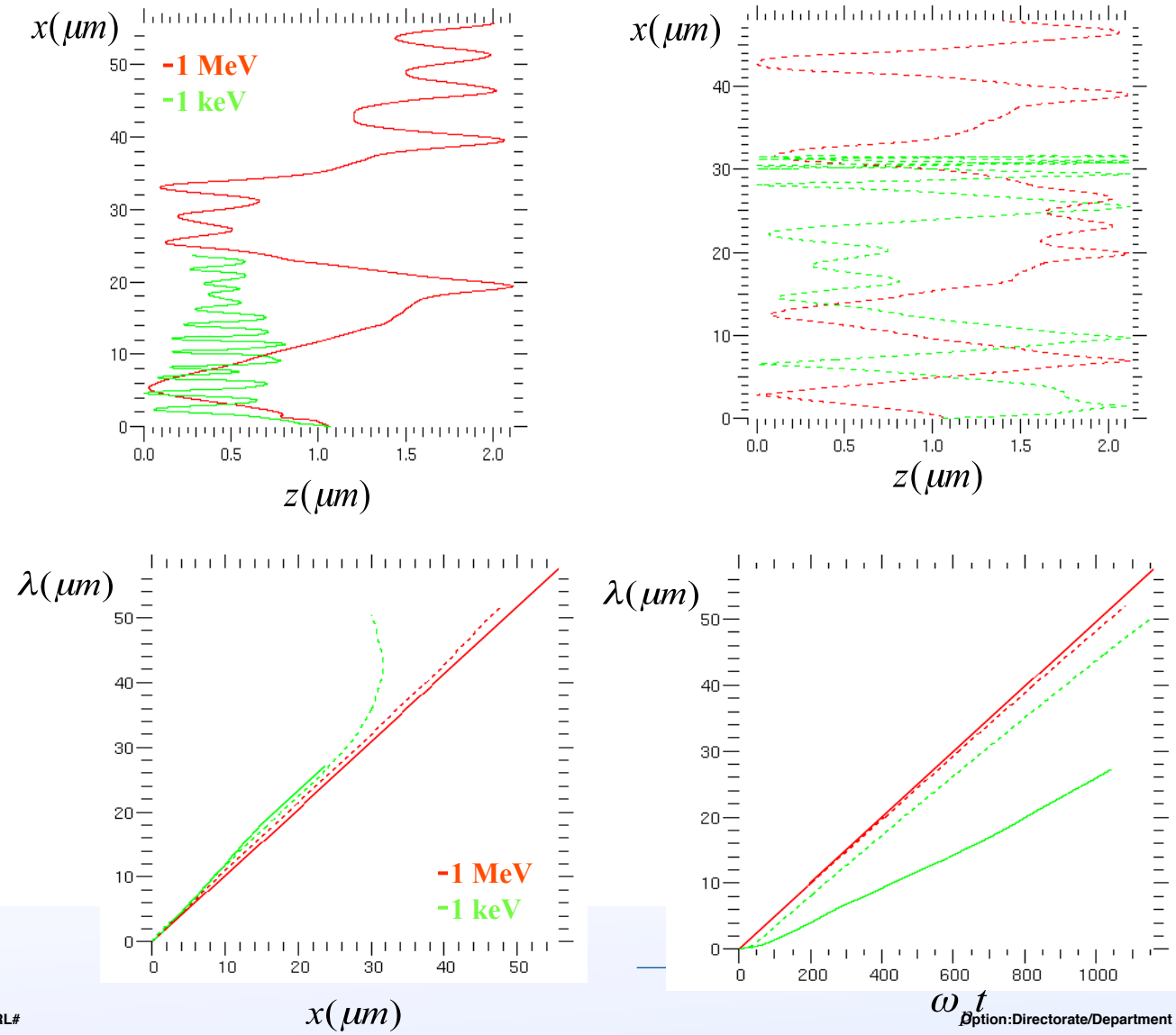

Fit trajectories/pathlengths

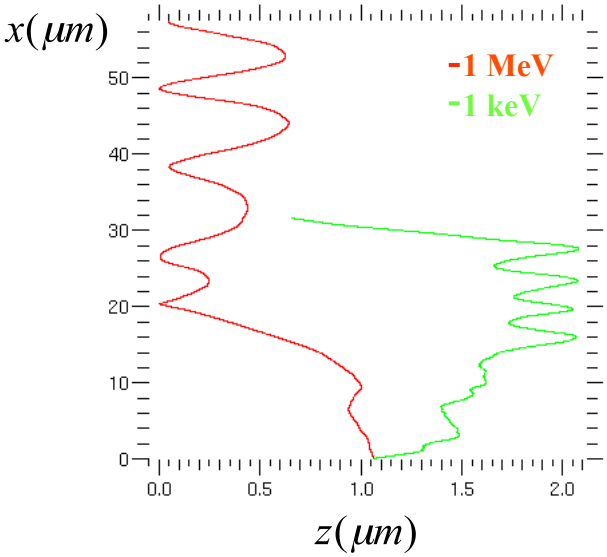

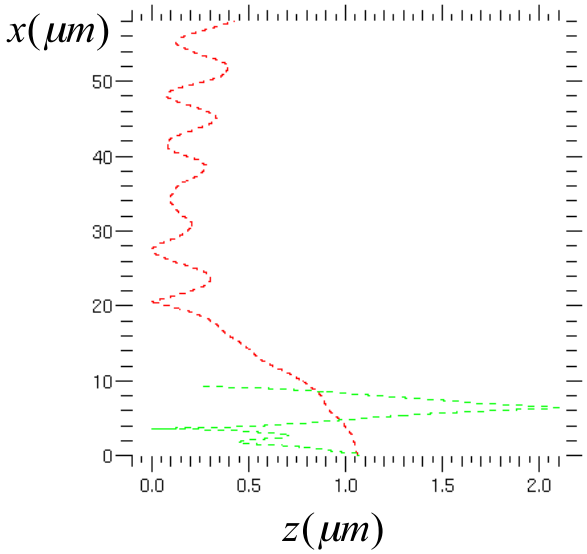

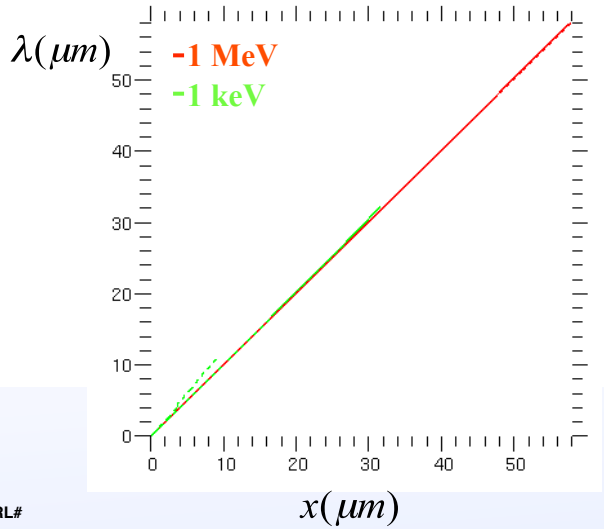

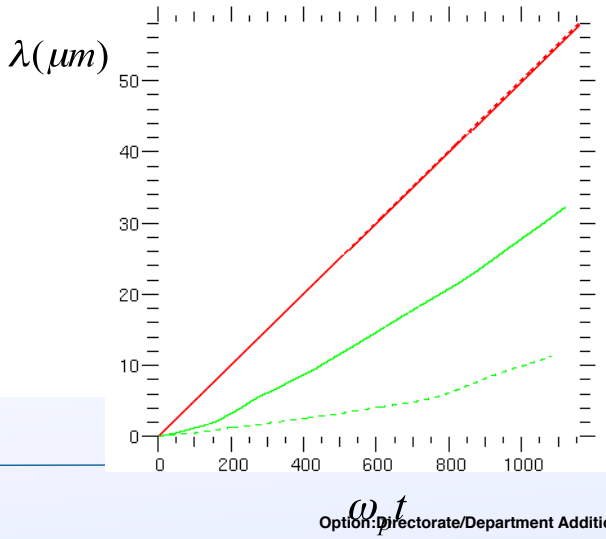

Filament hopping

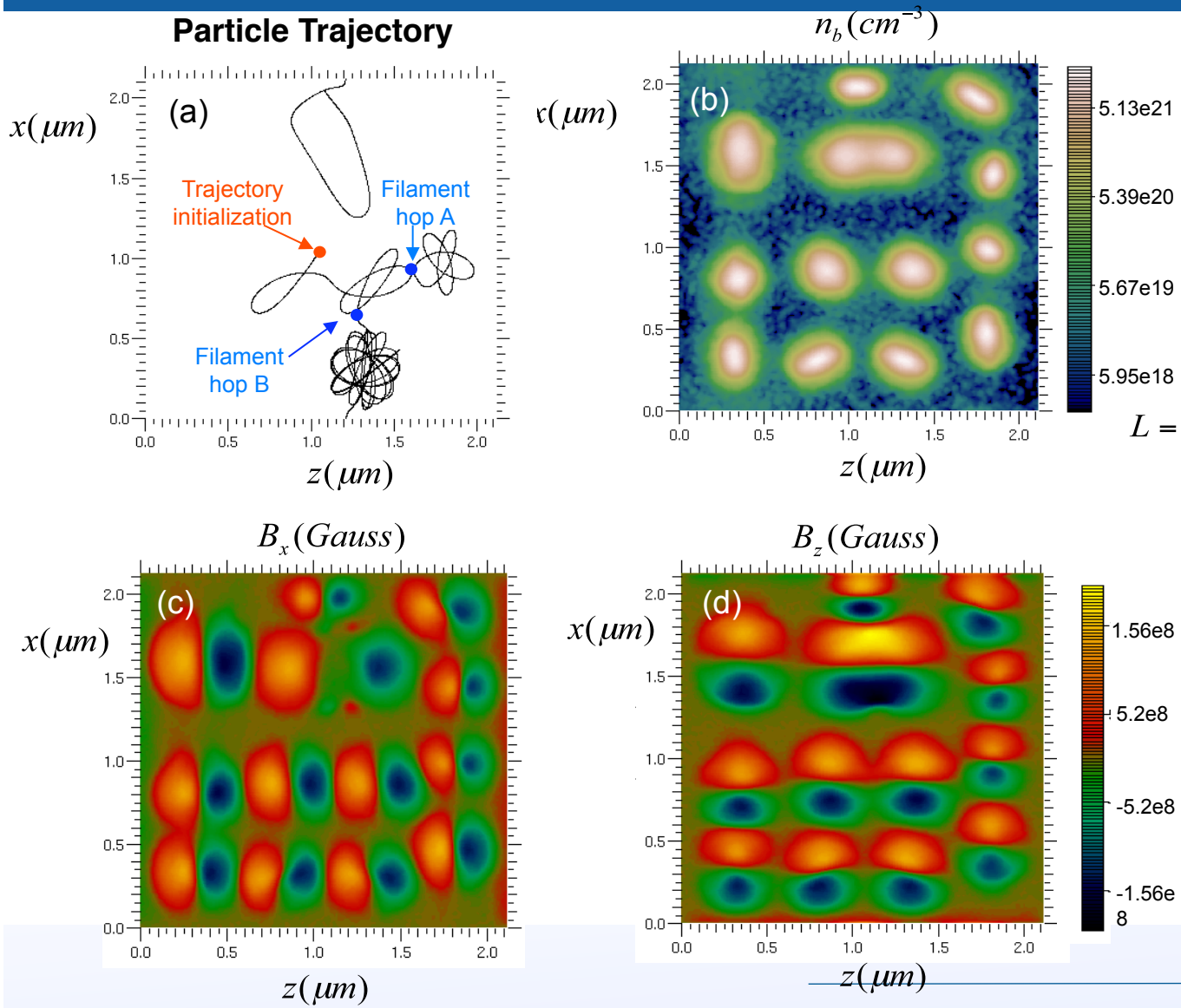

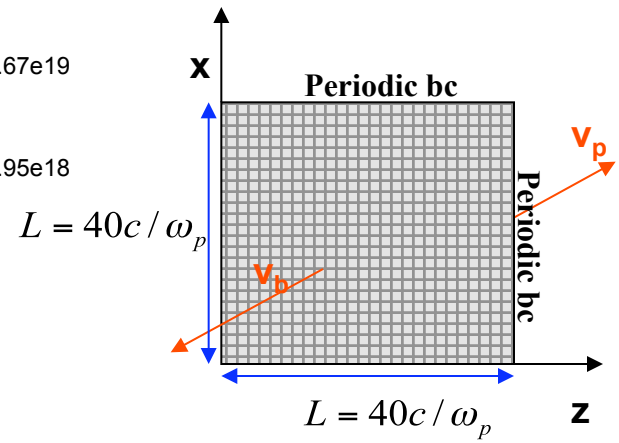

Filament hopping force analysis

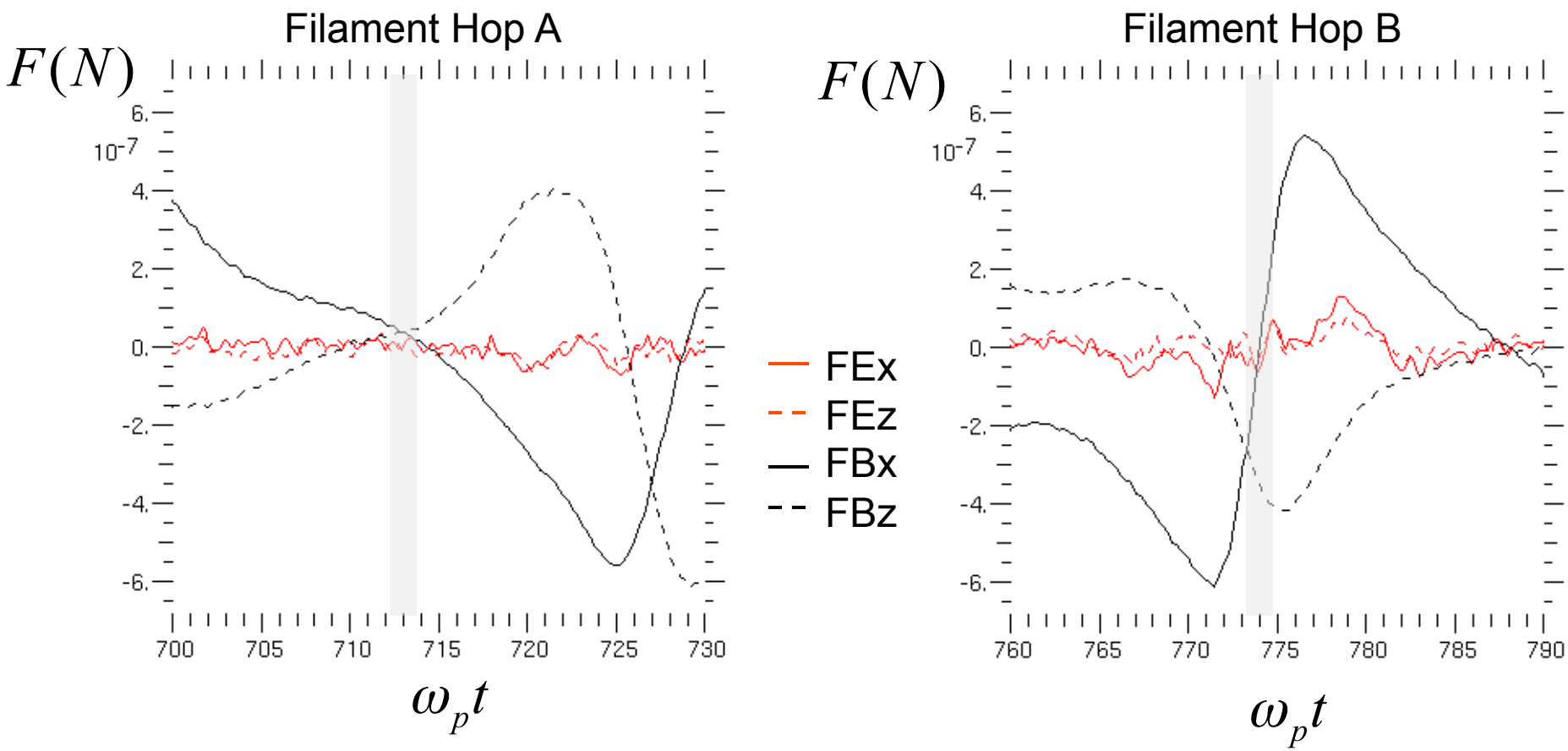

conclusions